Cancer Cell
Article

Targeted Expression of BikDD Eradicates Pancreatic Tumors in Noninvasive Imaging Models

Xiaoming Xie,[1] Weiya Xia,[1] Zhongkui Li,[2] Hsu-Ping Kuo,[1,4] Yuanfang Liu,[1] Zheng Li,[1] Qingqing Ding,[1] Su Zhang,[1] Bill Spohn,[1] Yan Yang,[1] Yongkun Wei,[1] Jing-Yu Lang,[1] Douglas B. Evans,[2] Paul J. Chiao,[1,2] James L. Abbruzzese,[3] and Mien-Chie Hung[1,2,4,*]
[1] Department of Molecular and Cellular Oncology
[2] Department of Surgical Oncology
[3] Department of Gastrointestinal Medical Oncology
The University of Texas M.D. Anderson Cancer Center, Houston, Texas 77030, USA
[4] Graduate School of Biomedical Sciences
The University of Texas Health Science Center, Houston, Texas 77030, USA
*Correspondence: mhung@mdanderson.org
DOI 10.1016/j.ccr.2007.05.009

SUMMARY

Pancreatic cancer is an aggressive malignancy with morbidity rates almost equal to mortality rates because of the current lack of effective treatment options. Here, we describe a targeted approach to treating pancreatic cancer with effective therapeutic efficacy and safety in noninvasive imaging models. We developed a versatile expression vector "VISA" (VP16-GAL4-WPRE integrated systemic amplifier) and a *CCKAR* (cholecystokinin type A receptor) gene-based, pancreatic-cancer-specific promoter VISA (CCKAR-VISA) composite to target transgene expression in pancreatic tumors in vivo. Targeted expression of *BikDD*, a potent proapoptotic gene driven by CCKAR-VISA, exhibited significant antitumor effects on pancreatic cancer and prolonged survival in multiple xenograft and syngeneic orthotopic mouse models of pancreatic tumors with virtually no toxicity.

INTRODUCTION

Pancreatic cancer is one of the most aggressive human malignancies, and approximately 37,170 new cases will be diagnosed in 2007 in the United States (Jemal et al., 2007). Despite efforts over the past three decades to improve diagnosis and treatment, the prognosis of patients with pancreatic cancer is extremely poor with or without treatment, and no effective markers have been found for early diagnosis or effective therapy. Nearly 50% of patients have metastatic diseases at diagnosis, and nearly 100% of patients develop metastases and die of the disease. The survival rates for patients with pancreatic cancer are the lowest of all cancers; the overall 5 year survival rate is less than 4%. At any stage, pancreatic cancer responds poorly to chemotherapy and radiation therapy. Management in most cases is palliative because chemotherapy and radiotherapy are not curative (Bardeesy and DePinho, 2002; Hingorani et al., 2005; Jaffee et al., 2002; Li et al., 2004). Therefore, an effective strategy for the treatment of pancreatic cancer is urgently needed.

At least two substantial obstacles exist in developing a safe and effective gene therapy strategy for treating pancreatic cancer, however—the lack of a pancreatic-cancer-specific expression vector with strong activity and stringent specificity and the lack of a convenient animal model for spatiotemporal monitoring of tumor growth and metastasis. Recently reported pancreatic-cancer-specific or

SIGNIFICANCE

Gene therapy for pancreatic cancer has been tested, but its development has been hampered by concerns with safety and efficacy and the limitations of conventional animal models. This report describes a robust pancreatic-cancer-specific expression vector, CCKAR-VISA, and its application in pancreatic tumor-bearing mouse models. Systemic administration of CCKAR-VISA-driven *BikDD*, a potent proapoptotic gene, in DNA:liposome complexes vigorously repressed growth of pancreatic tumors and metastasis and prolonged survival in multiple orthotopic mouse models. These findings constitute a strategy for potentially eliminating pancreatic cancer safely and effectively and highlight useful models for noninvasive spatiotemporal monitoring. The newly developed VISA system is also a versatile tool to boost other tissue- or cancer-specific promoters for developing promising therapeutics for other diseases.

cancer-specific promoters (Chen et al., 2004; Jacob et al., 2005; Li et al., 2006; Su et al., 2005; Wang et al., 2004; Wesseling et al., 2001) show much lower activity than the commonly used strong cytomegalovirus (CMV) enhancer/promoter, which is ubiquitously active. The efficacy of gene therapy depends greatly on the efficiency of transgene expression after systemic delivery. Therefore, one of our goals in the current study was to develop a pancreatic-cancer-specific expression vector that would not only maintain pancreatic cancer specificity but also produce robust activity, i.e., activity stronger than or comparable to that of the CMV promoter-driven expression vector, in pancreatic cancer cells but much lower activity in normal cells.

Bioluminescent imaging has been used to monitor the growth of solid tumors and lymphomas in the abdomen and to detect in vivo cell proliferation, signal transduction pathways, and apoptosis in animal models (El-Deiry et al., 2006; Gelovani Tjuvajev and Blasberg, 2003; Gross and Piwnica-Worms, 2005; Thorne et al., 2006; Xie et al., 2004). Recently, we generated an EZC-prostate model in which the prostate glows because of the expression of firefly luciferase in prostate epithelial cells (Seethammagari et al., 2006; Xie et al., 2004) and imaged targeted firefly luciferase activity in the endothelial cells of xenografts in vivo by using an IVIS imaging system (Xenogen, Alameda, CA) (Ou-Yang et al., 2006). The advantages of this imaging technique for pancreatic cancer gene therapy are its ability to monitor and allow optimization of gene therapy protocols and to detect the growth and metastases of pancreatic tumors in real time without having to kill the animals. In this study, we used pancreatic cancer cell lines (AsPC-1-Luc and Panc02-Luc) made to stably express firefly luciferase enzyme and established orthotopic pancreatic cancer xenograft models in which the growth and metastasis of the tumors can be noninvasively monitored by a live-animal imaging system.

All roads to successful eradication of cancer cells by nonsurgical modalities exploit the induction of apoptosis (Hanahan and Weinberg, 2000; Reed, 2003). The BH3-only group of the Bcl-2 family, central regulators of the mitochondrial pathway of apoptosis, serves as sentinels for cellular derangement (Boyd et al., 1995; Han et al., 1996). Of the BH3-only members (Bad, Bik, Noxa, HRK, Puma, BMF, Bid, and Bim), Bik (Bcl-2 interacting killer) in particular demonstrates not only the greatest binding affinity for Bcl-2 and Mcl-1 but also the broadest binding pattern (Bcl-2, Bcl-X_L, BCL-w, and Mcl-1) compared with the other BH3 members (Certo et al., 2006). We previously demonstrated that systemic delivery of the Bik gene by liposomes significantly inhibited the growth and metastasis of human breast cancer in nude mice (Zou et al., 2002). Bik expression by adenovirus has also been reported to trigger apoptosis of human malignant glioma cells in vivo (Naumann et al., 2003). More recently, we developed a Bik mutant (BikDD) in which changes were made in T33D and S35D to mimic phosphorylation at these two residues, enhancing their binding affinity with the antiapoptotic proteins Bcl-X_L and Bcl-2. This mutant was more potent than Bik wild-type and other Bcl-2 family proapoptotic genes, such as Bad, Bak, and Bok, in inducing apoptosis and inhibiting cell proliferation in various human cancer cells (Chen et al., 2004; Day et al., 2006; Li et al., 2003).

Thus, our purpose in undertaking this study was threefold: to develop an active, pancreatic-specific expression vector for delivering the apoptotic gene *BikDD* specifically to pancreatic cancer cells; to test the effectiveness of this expression vector in the orthotopic mouse models of pancreatic cancer; and to demonstrate the feasibility of imaging the gene delivery and its aftermath in real time in living animals.

RESULTS

The Molecularly Engineered CCKAR-Based Expression Vector, C-VISA, Is Robust, Specific to Pancreatic Cancer Cells, and Prolongs Transgene Expression

CCKAR has been shown to be overexpressed in human pancreatic ductal adenocarcinomas (PDAC) or human PDAC cell lines compared to normal human pancreatic ductal epithelium (HPDE) (Goetze et al., 2000; Jang et al., 2005; Moonka et al., 1999; Weinberg et al., 1997). We also examined the CCKAR expression in nine human PDAC specimens from patients and found that the endogenous CCKAR mRNA was overexpressed in 77.7% (7 of 9) of the human PDAC tumors but undetectable in the human normal pancreatic tissue (see Figure S1A in the Supplemental Data available with this article online), consistent with reports from several independent groups as indicated above. We have also previously shown that the CCKAR promoter is selectively active in pancreatic cancer cells as compared with other normal cell lines (Li et al., 2006). Although the CCKAR promoter is active in and specific to pancreatic cancer cells, its activity is less than 0.3% of that of the CMV promoter (Figure 1B). Such low activity would lead to very poor efficacy in gene therapy settings (Conwell and Huang, 2005; Qiao et al., 2002; Reynolds et al., 2001; Xie et al., 2001). To enhance the efficiency of its pancreatic-cancer-specific expression, we first engineered one copy of the 0.8-kb WPRE (the posttranscriptional regulatory element of the woodchuck hepatitis virus) (Glover et al., 2002; Zufferey et al., 1999) downstream of the luciferase gene to posttranscriptionally regulate luciferase gene expression, producing the plasmid CCKAR-Luc-WPRE (C-P-Luc) (Figure 1A). The activity of C-P-Luc in the PDAC cell lines AsPC-1, PANC-1, and Panc02 was increased by 3.9-, 2.6-, and 3.1-fold, respectively, compared with the CCKAR promoter (Figure 1B). However, as compared with the CMV promoter, the C-P-Luc promoter was still too weak. Because the two-step transcriptional amplification (TSTA) system can significantly amplify the activity of the prostate-specific antigen (PSA) promoter (Iyer et al., 2001; Zhang et al., 2003), we reasoned that the activity of the CCKAR promoter could be augmented by using the TSTA system. To test this hypothesis, we generated the plasmid CCKAR-TSTA-Luc (C-T-Luc) (Figure 1A).

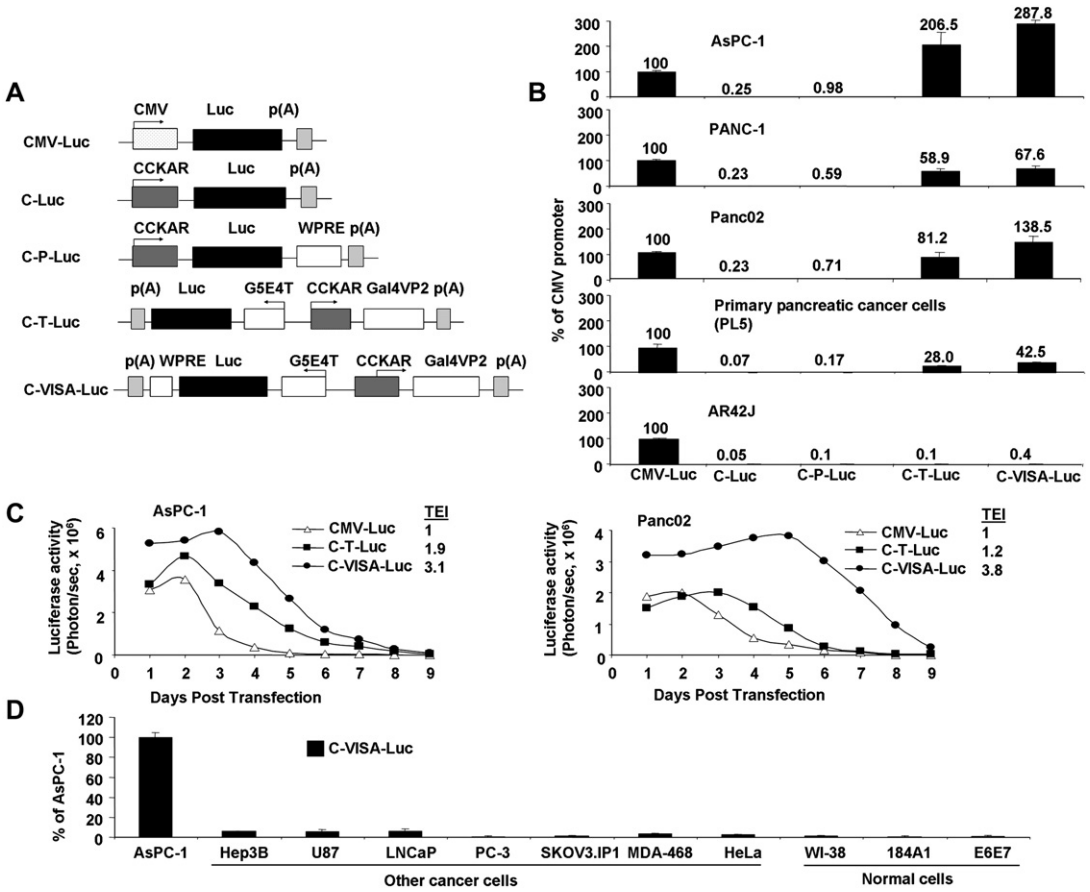

Figure 1. Molecularly Engineered CCKAR-Based Promoter C-VISA Is Robust, Prolongs Duration of Gene Expression, and Is Pancreatic Cancer Specific

(A) Schematic diagram of engineered CCKAR-based constructs.

(B) Activity of CCKAR-based promoters in pancreatic cancer cells and pancreatic acinar cells. The data represent the mean of four independent experiments. Error bars indicate SD.

(C) Kinetics of luciferase activity driven by CMV, C-TSTA, or C-VISA promoter. AsPC-1 and Panc02 cells were transiently transfected with the indicated plasmid DNA and were imaged with the IVIS imaging system. The photon signals (photons/sec) of luciferase expression were plotted. The data represent the mean of two independent experiments. TEI, total expression index.

(D) Tissue specificity of the C-VISA promoter. Shown is the percentage of the dual luciferase ratio for each cell line relative to the dual luciferase ratio for AsPC-1 cells which is set at 100%. The data represent the mean of four independent experiments. Error bars indicate SD.

Indeed, the TSTA system dramatically amplified the CCKAR promoter activity in AsPC-1, PANC-1, and Panc02 cells (826-, 256-, and 353-fold increases, respectively, in comparison with the activities of the CCKAR promoter) (Figure 1B). To generate a more active expression vector based on these findings, we then combined the WPRE element into the TSTA system to produce a VISA (VP16-Gal4-WPRE integrated systemic amplifier) system. The CCKAR promoter was fused to the VISA system to produce CCKAR-VISA (C-VISA) (Figure 1A). Luciferase activity with the C-VISA promoter was increased by 1140-, 297-, and 600-fold in AsPC-1, PANC-1, and Panc02 cells, respectively, relative to the CCKAR promoter alone (Figure 1B). Overall, the C-VISA activity reached 287.8%, 67.6%, and 138.5% of the activity of the CMV promoter in AsPC-1, PANC-1, and Panc02 cells, respectively, at 2 days after transfection (Figure 1B). To ensure the generality of C-VISA for high-level expression in human PDAC, we further examined the activities of these constructs in 11 more human PDAC cell lines available. As shown in Figure 1B and Figure S1B, C-VISA exhibited a general strong activity in all 13 human PDAC cell lines tested, with a 557-, 152- and 1.5-fold increase as compared with CCKAR(C), CCKAR-WPRE (C-P), and CCKAR-TSTA (C-T), respectively. On average, the C-VISA activity was as high as 85.5 ± 21.7% of the CMV activity in all 13 human PDAC cell lines (Figure 1B and Figure S1B). Importantly, the C-VISA vector was also robust in the primary cultured pancreatic cancer cells (PL5), with 42.5% of the CMV promoter and resulting in a 607-, 250-, and 1.50-fold increase as compared with C, C-P, and C-T, respectively (Figure 1B). To ensure that C-VISA is not active in pancreatic acinar cells, we further measured the activity of C-VISA in the pancreatic acinar cell line AR442J (Sata et al., 1999).

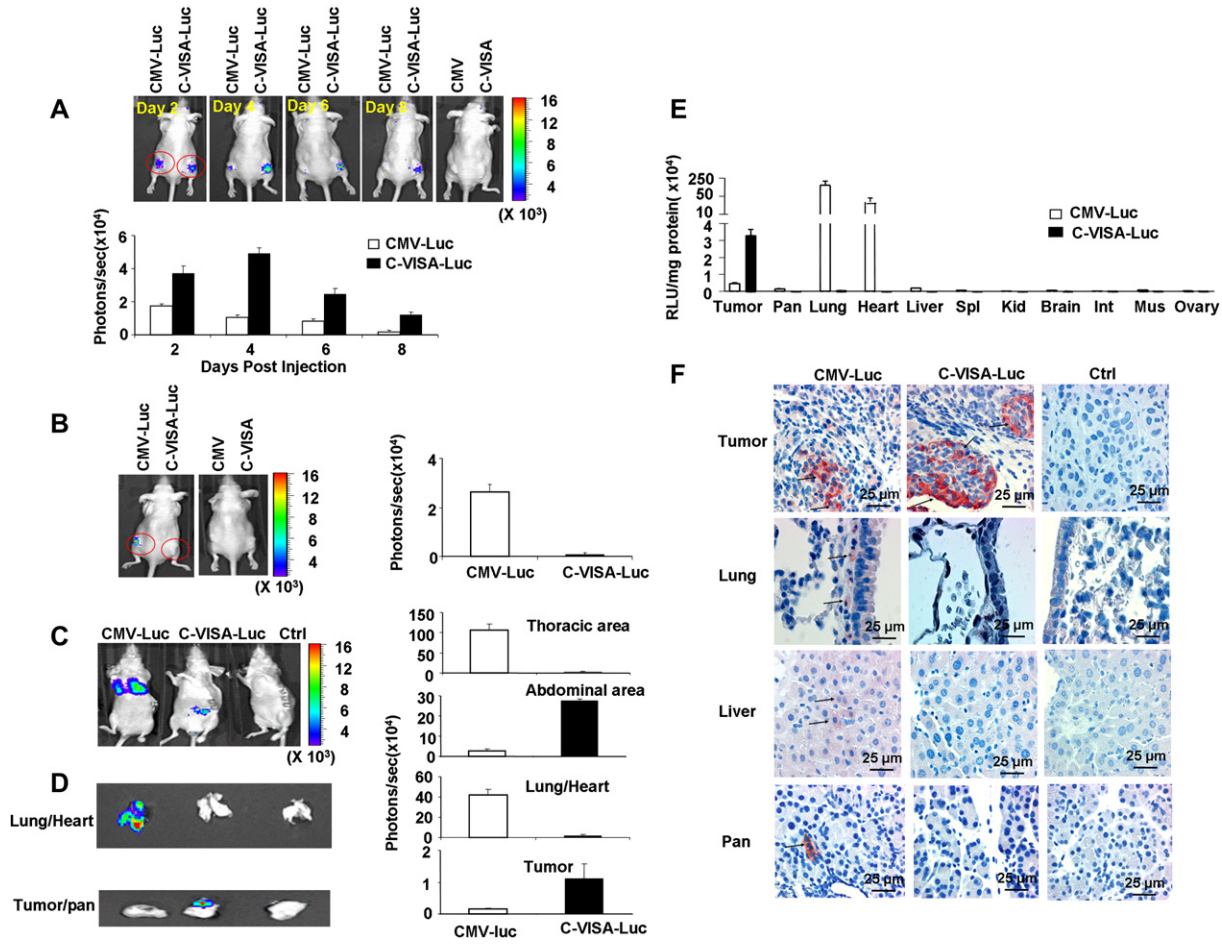

Figure 2. C-VISA Transcriptionally Targets Transgene Expression to Pancreatic Cancer in Animal Models

(A) Luciferase expression driven by the C-VISA promoter is more robust and more persistent in AsPC-1 tumors. Subcutaneous AsPC-1 tumors in nude mice were intratumorally injected with 50 μg of liposomal plasmid DNA. Shown are representative images (upper panel) from each group of four mice and the quantified photon signals (photons/s) (lower panel). Error bars indicate SEM.

(B) Luciferase expression driven by C-VISA promoter is undetectable in Hep3B tumors. Hep3B tumors in nude mice were intratumorally injected as described in (A). Mice underwent imaging 2 days after injection. Shown are representative images (left panel) from each group of four mice and the quantified photon signals (photons/s) (right panel). Error bars indicate SEM.

(C–F) The C-VISA promoter targets the luciferase expression to pancreatic cancer in an orthotopic model of AsPC-1 tumors after systemic administration. Nude mice bearing orthotopic AsPC-1 tumors were intravenously injected with 50 μg of liposomal DNA. Mice were subjected to in vivo imaging (C). The lungs/hearts and pancreata with tumors from mice from (C) were subjected to ex vivo imaging (D). The photon signals were quantified (shown on the right). Tissue specimens from tumors and specified organs dissected from mice in (C) at 2 days after systemic delivery were measured for luciferase activity with a luminometer (E). The data are expressed as relative light units (RLU) per milligram of total protein. Tissue specimens from (E) were fixed and processed for immunohistochemical analysis of firefly luciferase expression [(F) and data not shown]. Error bars indicate SD; Pan, pancreas; Spl, spleen; Kid, kidney; Inte, intestine; Mus, muscle.

The data showed that the C-VISA activity was as low as 0.4% of the CMV promoter activity in AR42J cells (Figure 2B), suggesting that it may remain very low in the pancreatic acini, thus, in favor of its application to gene therapy for pancreatic cancer. Because WPRE increases the half-life of the RNA transcripts (Zufferey et al., 1999), we reasoned that WPRE in the C-VISA vector might prolong the duration of transgene expression. To test this, we measured the kinetics of the luciferase activity in AsPC-1 and Panc02 cells after transient transfection. Indeed, C-VISA significantly prolonged the duration of luciferase gene expression in both cell lines (Figure 1C). For instance, on the fifth day after transfection, the activity of luciferase induced by the CMV promoter had almost completely disappeared, whereas the activity induced by C-VISA was still robust in both cell lines. The total expression index (TEI) of C-VISA (in comparison with the area under the curve of luciferase activity in Figure 1C, with CMV activity set as 1) was 3.1 in AsPC-1 cells and 3.8 in Panc02 cells. The significantly improved TEI of the therapeutic gene should further improve the efficacy of gene therapy. Most importantly, C-VISA remained low in nonpancreatic cancer cells (liver, prostate, ovary, breast, uterine cervix, and brain) and in normal cells from the lung, breast, or

pancreatic epithelium (Figure 1D), all of which must be protected during systemic delivery of suicide or proapoptotic genes. Thus, the engineered promoter composite C-VISA produced expression activity that was 3- to 4-fold higher than that of the CMV promoter (as measured by the TEI) in the pancreatic cancer cells tested; the composite prolonged gene expression in vitro; and the gene expression remained low in nonpancreatic cancer cells and normal cells. This C-VISA vector should be ideal for targeting a therapeutic gene to treat pancreatic cancer in a gene therapy setting.

C-VISA Transcriptionally Targets Transgene Expression in Pancreatic Cancer in Mouse Models

To determine whether the activity and specificity of C-VISA can also be maintained in vivo, we next evaluated the activity and expression of firefly luciferase driven by C-VISA using the IVIS imaging system and immunohistochemical analysis after intratumoral and intravenous systemic delivery of the plasmid DNA:liposome complexes in mice (Chen et al., 2004; Day et al., 2006; Li et al., 2003; Templeton et al., 1997). First, to test the level and duration of gene expression driven by C-VISA, CMV-Luc:liposome or C-VISA-Luc:liposome complexes were injected into the AsPC-1 tumors on the right and left flanks of nude mice. The CMV (the plasmid containing the CMV enhancer/promoter without Luc) and C-VISA (plasmid containing the C-VISA promoter without Luc):liposome complexes were used as negative controls. Bioluminescent imaging showed that expression of the transgene firefly luciferase was induced rapidly after injection of the CMV-Luc:liposome complex, reached a peak on day 2, and then decreased sharply thereafter (Figure 2A). However, the expression of firefly luciferase induced by C-VISA-Luc was significantly stronger and lasted longer than that induced by CMV-Luc, reaching its peak on day 4 and lasting as long as 14 days (Figure 2A and data not shown). Consistent with the in vitro data (Figure 1C), the TEI of C-VISA in vivo was substantially higher than that of CMV (3.2 versus 1). Second, to investigate the specificity of gene expression driven by C-VISA, C-VISA-Luc:liposome and CMV-Luc:liposome complexes were injected into Hep3B (liver) tumor implants on the right and left flanks of nude mice. Imaging showed that signal was undetectable in the tumors treated with C-VISA-Luc complexes, whereas it was strong in the tumors treated with CMV-Luc (Figure 2B). Immunohistochemical analysis confirmed that C-VISA induced stronger expression of firefly luciferase in AsPC-1 tumors than did CMV-Luc (Figure S2A) and undetectable expression of luciferase in Hep3B tumors (Figure S2B).

Because our ultimate goal is to develop systemic gene therapy for pancreatic cancer, we also evaluated the expression pattern of transgene driven by C-VISA in several normal tissues after systemic delivery of plasmid DNA:liposome complexes. To this end, C-VISA-Luc:liposome and CMV-Luc:liposome complexes were intravenously injected into mice bearing AsPC-1 pancreatic tumors. Bioluminescent imaging revealed a strong signal in the thoracic area (lungs and heart) of mice treated with CMV-Luc (Figure 2C). This finding indicated that after systemic delivery, the complexes flowed through the circulatory system, remaining mostly in the lungs and heart, and luciferase was expressed because of the nonspecificity of the CMV promoter. In contrast, a signal was almost undetectable in the thoracic area but was detected in the abdomen of mice treated with C-VISA-Luc, indicating that C-VISA targeted luciferase expression to the AsPC-1 tumors after systemic delivery of the plasmid C-VISA-Luc DNA:liposome complexes.

To more unambiguously determine the source of the signal, the animals were humanely killed immediately after in vivo imaging as described above and their organs were dissected for ex vivo imaging. As shown in Figure 2D, the lungs and hearts of mice treated with CMV-Luc produced strong photon signals, causing the spots on the thoracic area. The spots in the abdominal area were shown to be from the pancreatic tumors of mice treated with C-VISA-Luc. To further determine the tissue distribution of transgene expression, tissue specimens from the tumors and major organs of the treated mice were harvested and tested for luciferase activity with a luminometer. Consistent with the in vivo and ex vivo imaging results, luciferase activity in the tumors of mice treated with C-VISA-Luc was 7.2-fold greater than that in the tumors of mice treated with CMV-Luc ($p < 0.01$) (Figure 2E). In contrast, the luciferase activity in the lungs and hearts of mice treated with CMV-Luc was 1299- and 2314-fold, respectively, greater than that in mice treated with C-VISA-Luc ($p < 0.0001$). The cancer-specific index (i.e., luciferase activity in the tumor compared with luciferase activity in the lungs) (Chen et al., 2004) was 47.7 for C-VISA-Luc and 0.005 for CMV-Luc. These findings indicate that C-VISA resulted in a 9500-fold improvement in the selectivity of transgene expression for tumor versus the usual site of vector sequestration, the lung, after systemic administration compared with the CMV promoter.

As mentioned earlier, a major determinant of the success of cancer gene therapy is the ability to obtain sufficient efficiency and specificity of transfection (Conwell and Huang, 2005; Lo et al., 2005; Qiao et al., 2002), particularly for systemic nonviral delivery (Glover et al., 2005). To determine the in vivo efficiency of systemic administration, tissue specimens from the tumors and major organs of mice were fixed, sectioned, and stained for luciferase expression using an anti-Luc antibody. Firefly luciferase protein staining demonstrated 22% ± 3% of tumor cells for in vivo luciferase expression in orthotopic AsPC-1 tumors of mice treated with C-VISA-Luc by intravenous injection, a slightly higher percentage than CMV-Luc (18% ± 2.6%) (Figure 2F). The staining signals of C-VISA-Luc, however, were much stronger than those of CMV-Luc. The evidence of in vivo luciferase expression analyzed by immunohistochemistry was consistent with the findings from the bioluminescent imaging and the luciferase activity assay (Figures 2C, 2D, and 2E), showing that intravenous treatment with CMV-Luc led to luciferase expression in the lung (luciferase positive cells 18% ± 3%), liver

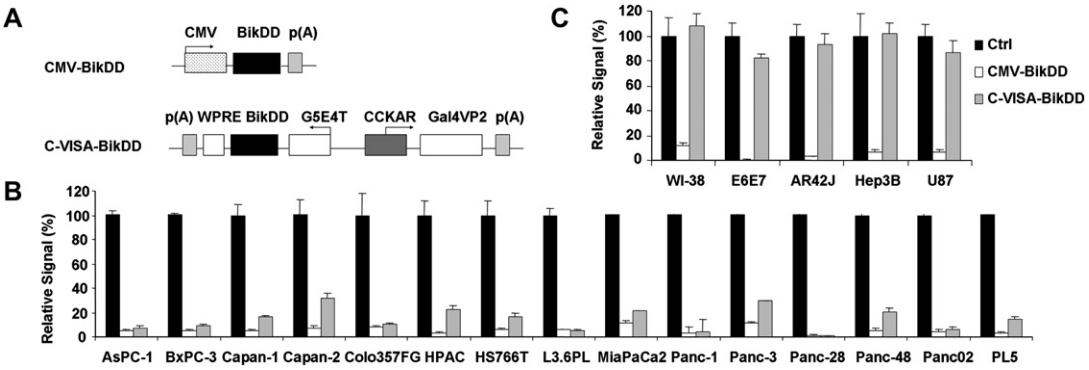

Figure 3. Expression of BikDD Driven by C-VISA Kills Pancreatic Cancer Cells Effectively and Specifically In Vitro

(A) Schematic diagram of expression constructs in the pUK21 backbone.

(B) BikDD expression driven by C-VISA kills PDAC cells effectively. The percentage of the signals as compared with the negative control (setting at 100%) was presented. The data represent the mean of three independent experiments. Error bars indicate SD.

(C) BikDD expression driven by C-VISA does not kill nonpancreatic cancer cells and normal cells. Error bars indicate SD.

(10% ± 2%), and pancreas (1% ± 0.5%), whereas treatment with C-VISA-Luc led to almost undetectable expression in these normal organs (Figure 2F). The results show that the molecularly engineered CCKAR promoter composite C-VISA transcriptionally targets transgene expression to pancreatic cancer in animal models. Thus, the C-VISA vector could be an excellent candidate for the development of a targeted, safe, and effective systemic gene therapy system for patients with pancreatic cancer.

Expression of BikDD Driven by the C-VISA Promoter Induces Death of Pancreatic Cancer Cells Effectively and Specifically In Vitro

To examine whether the C-VISA vector can deliver a therapeutic gene to selectively kill pancreatic cancer cells, we generated a therapeutic plasmid in the pUK21 backbone, pUK21-C-VISA-BikDD, in which the C-VISA vector drives BikDD expression (Figure 3A). pUK21-CMV-BikDD was used as a positive control (Figure 3A). To address the generality of C-VISA-BikDD for killing human PDAC, we tested the killing effects of C-VISA-BikDD on 13 human PDAC cell lines, one mouse PDAC cell line (Panc02), and one sample of primary cultured human PDAC cells (PL5) from a patient. Cells were transiently cotransfected with pUK21-CMV-BikDD, pUK21-C-VISA-BikDD, or pUK21-C-VISA (negative control) plus pGL3-CMV-Luc (the indicator control). Cell killing effects were monitored with the IVIS imaging system. C-VISA-BikDD effectively killed all 13 human PDAC cell lines, the mouse PDAC cell line, and the primary cultured human PDAC cells, as comparable with the CMV-BikDD (Figure 3B). However, C-VISA-BikDD did not kill nonpancreatic cancer cells Hep3B (liver), U87 (brain), and normal lung fibroblasts WI-38, normal HPDE cells E6E7, and rat pancreatic acinar cells AR42J (Figure 3C). In contrast, CMV-BikDD induced death of not only pancreatic cancer cells (Figure 3B) but also all nonpancreatic cancer cells and normal cells tested (Figure 3C). Thus, C-VISA-driven BikDD selectively kills pancreatic cancer cells in vitro.

C-VISA-BikDD Represses Tumor Growth More Effectively Than CMV-BikDD in Orthotopic Models of AsPC-1-Luc and Colo357FG Xenografts

To evaluate the antitumor effects of C-VISA-BikDD on human pancreatic cancer in vivo, we first treated immunodeficient mice bearing orthotopic xenografts of human pancreatic cancer cells (tumors were 100–150 mm^3 [as measured postmortem with calipers], corresponding to 1.4×10^7 photons/tumor/second [as measured with the IVIS imaging system] with systemic delivery of liposomal C-VISA-BikDD complexes). Nude mice bearing the orthotopic AsPC-1-Luc pancreatic tumors were treated with doses of 5 μg, 15 μg, or 45 μg of C-VISA-BikDD or 45 μg of C-VISA (Ctrl) in a liposomal complex via tail-vein injection, twice per week for 3 weeks (six applications total) based on the expression pattern and transfection efficiency of luciferase reporter gene in vivo described above. Tumors were noninvasively monitored in vivo with the IVIS imaging system. Compared with the control, treatment with C-VISA-BikDD significantly reduced signal from the tumors in a dose-dependent manner (Figure 4A).

To compare the antitumor effects of C-VISA-BikDD with those of CMV-BikDD, nude mice bearing AsPC-1-Luc tumors were given 15 μg of CMV-BikDD, C-VISA-BikDD, or C-VISA (Ctrl) in a liposomal complex via tail vein injection, twice per week for 3 weeks. Imaging revealed that treatment with either CMV-BikDD or C-VISA-BikDD led to significantly decreased signal from the tumors 1 week after starting treatment (both $p < 0.0001$ versus control) (Figure 4B). Furthermore, C-VISA-BikDD decreased the signal to a greater extent than did CMV-BikDD ($p < 0.05$ on day 21 and $p < 0.01$ on day 28), indicating that C-VISA-BikDD inhibited growth of human-derived pancreatic cancer more effectively than did CMV-BikDD (Figure 4B). CMV-BikDD also prolonged the median survival time of mice compared with the control (52 ± 8 days versus 31 ± 4 days, $p < 0.004$). Moreover, C-VISA-BikDD prolonged survival more effectively than did CMV-BikDD ($p < 0.01$) (Figure 4C). Signal was undetectable in five of eight mice

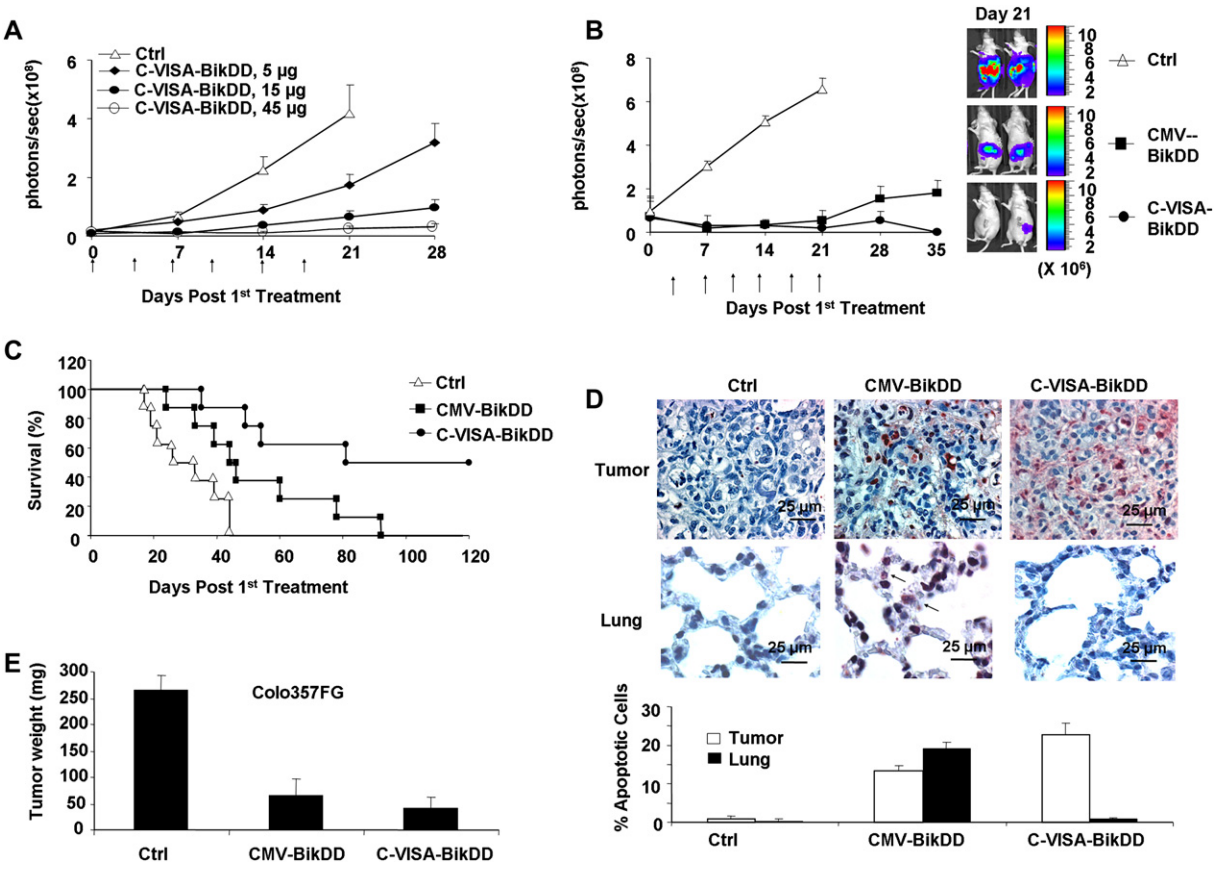

Figure 4. Expression of BikDD Driven by C-VISA Promoter Inhibits Tumor Growth and Prolongs Mouse Survival More Effectively Than That Driven by CMV Promoter in Orthotopic Xenograft Models

(A) Expression of BikDD driven by C-VISA promoter inhibited tumor growth in a dose-dependent manner. Nude mice bearing AsPC-1-Luc tumors were systemically given liposomal plasmid DNA at indicated doses (n = 8 mice/group). The photon signals were quantified with Xenogen's living imaging software. Error bars indicate SEM.

(B–D) Expression of BikDD driven by C-VISA promoter inhibited human pancreatic tumor growth of AsPC-1 and prolonged mouse survival more effectively than BikDD driven by CMV promoter. Nude mice bearing AsPC-1-Luc tumors were intravenously injected with 15 μg of liposomal plasmid DNA as above (n = 8 mice/group). (B) The photon signals (left panel) were quantified with Xenogen's living imaging software and representative images are shown (right panel). Error bars indiacte SEM (C) Kaplan-Meier survival analysis was performed. Data shown are representative of two separate experiments. (D) In vivo apoptosis of tissue specimens was analyzed. The percentages of apoptotic cells from five fields of the indicated tissues are shown (lower panel). (E) Expression of BikDD driven by C-VISA promoter inhibited human pancreatic tumor growth of Colo357FG. Two weeks after the last treatment, mice were killed, and the tumors were dissected and weighed. Error bars indicate SD.

(62.5%) at 60 days after treatment in the C-VISA-BikDD group. After 14 months, four of those five mice treated with C-VISA-BikDD still showed no detectable signal, suggesting that tumors did not recur. To assess apoptosis in vivo after treatment, 2 days after the second administration of the BikDD complexes three mice per group were killed and their tumors sectioned for apoptosis detection by terminal deoxynucleotidyl transferase [TdT]-mediated dUTP nick end labeling (TUNEL) assay. Both C-VISA-BikDD and CMV-BikDD induced substantial tumor cell apoptosis. However, CMV-BikDD also led to remarkable apoptosis in the lung tissue, but C-VISA-BikDD did not (Figure 4D), indicating that C-VISA induced BikDD expression in the targeted pancreatic tumor cells but not in the normal tissues such as lungs. Consistent with the tumor growth and mouse survival results, C-VISA-BikDD showed more potent apoptosis than did CMV-BikDD ($p < 0.007$) (Figure 4D). To examine the antitumor effects of C-VISA-BikDD in multiple models, we further investigated the in vivo repression of Colo357FG and Colo357L3.6pl tumor growth by systemic administration of C-VISA-BikDD in orthotopic nude mouse models. BALB/c *nu/nu* nude mice bearing Colo357FG or Colo357L3.6pl tumors were treated as described above. The mice were killed and the tumors were dissected and weighed 2 weeks following the last treatment. We found that systemic administration of liposomal C-VISA-BikDD vector inhibited human pancreatic tumor growth of Colo357FG ($p < 0.001$, versus Ctrl) (Figure 4E) and of Colo357L3.6pl ($p < 0.01$, versus Ctrl) (Figure S3). It is worthwhile to mention that even the expression level of luciferase driven by C-VISA is slightly lower than that by the CMV promoter in

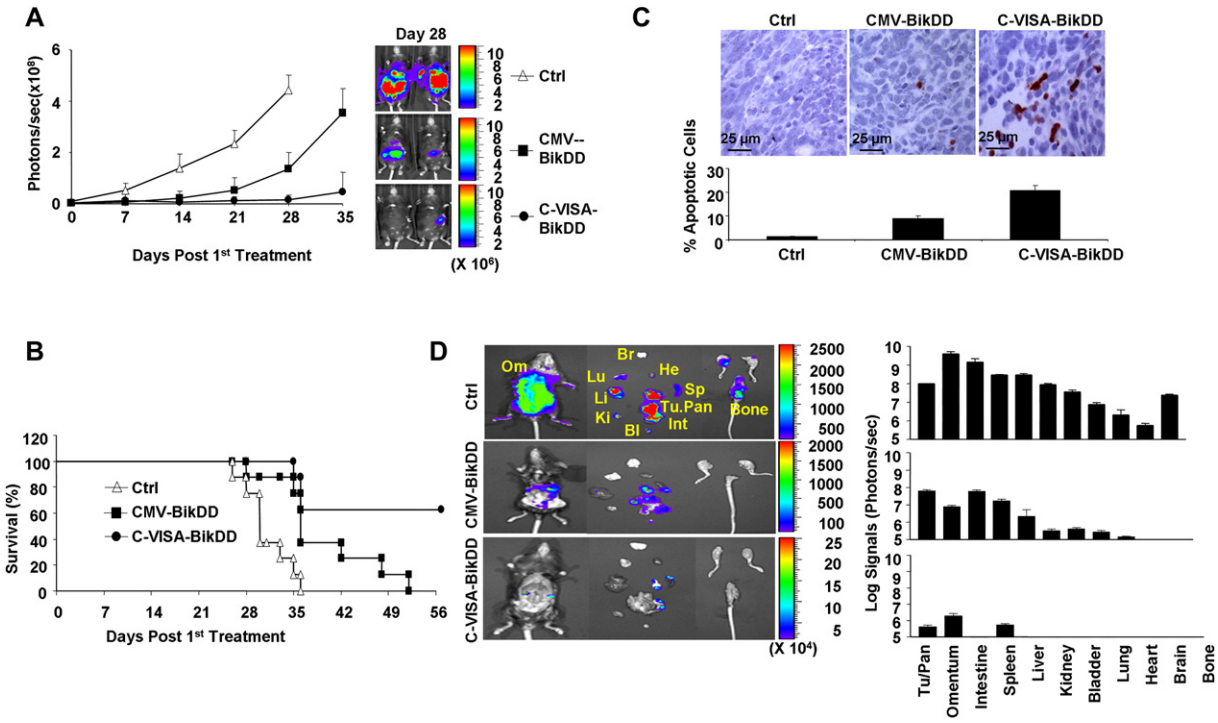

Figure 5. Expression of BikDD Driven by C-VISA Promoter Inhibits Tumor Growth and Invasion/Metastasis and Prolongs Mouse Survival More Effectively Than That Driven by CMV Promoter in an Orthotopic Syngeneic Model

(A–C) Expression of BikDD driven by C-VISA promoter inhibited tumor growth and prolonged mouse survival more effectively than BikDD driven by CMV promoter. C57BL/6 mice bearing Panc02-Luc tumors were treated as described above and were subjected to in vivo imaging. (A) The photon signals were quantified with Xenogen's software (n = 8 mice/group) and representative images are shown (right panel). Error bars indicate SEM. (B) Kaplan-Meier survival analysis from (A). (C) In vivo apoptosis of tissue specimens was analyzed. The percentages of apoptotic cells from five fields of the indicated tissues are shown (lower panel). Error bars indicate SD.

(D) C-VISA-BikDD inhibits invasion/metastasis of Panc02 tumors in an orthotopic syngeneic model. The mice with Panc02 tumors were treated as described in Figure 6A and subjected to in vivo imaging on day 28 after the first treatment. The mice were then killed, the dissected tumors and organs were imaged ex vivo (left panels), and the signals were quantified (right panels). Error bars indicate SEM; Tu, tumor; Pan, pancreas; Tu/Pan, tumor and/or pancreas.

Colo357L3.6pl pancreatic cancer cell line based on the luciferase activity 2 days after transfection (Figure S1B), the therapeutic efficacy of C-VISA-BikDD tested in the xenograft model is slightly better than or at least comparable to that of CMV-BikDD. This may be due to the fact that the C-VISA vector prolongs expression of the transgene resulting in increased TEI (Figure 1C) and therapeutic efficacy should be more related to the TEI than to the expression level on a particular day (Figure 1B and Figure S1B). Thus, C-VISA-BikDD induced targeted apoptosis, repressed tumor growth in a dose-dependent manner, and suppressed tumor growth more effectively than did CMV-BikDD in multiple orthotopic models of human pancreatic cancer.

C-VISA-BikDD Inhibits Tumor Growth and Metastasis and Prolongs Mouse Survival More Effectively Than CMV-BikDD in an Orthotopic Syngeneic Model of Panc02-Luc Tumor

Because nude mice are immunodeficient, the nude mouse xenograft model cannot be used to address the role of the immune system in affecting tumor growth and repeated plasmid administration. These issues will be important clinically if the therapeutic efficacy of C-VISA-BikDD can be examined in an intact immunocompetent mouse model. To this end, we explored use of a syngeneic mouse pancreatic tumor model (Yan et al., 2006). Female C57BL/6 mice bearing established orthotopic Panc02-Luc tumors (100–150 mm^3 [as measured postmortem with calipers], corresponding to 5×10^6 photons/tumor/second [as measured with the IVIS imaging system]) were treated as described above. In contrast to the control mice, in which the strength of signals increased over time, the signals from mice treated with CMV-BikDD or C-VISA-BikDD were much weaker just 14 days after the first treatment ($p < 0.01$ and $p < 0.009$, respectively, versus Ctrl) (Figure 5A). As in the xenograft model, C-VISA-BikDD decreased the signals to a greater extent than did CMV-BikDD ($p < 0.05$ on day 21 and $p < 0.02$ on day 28), indicating that C-VISA-BikDD inhibited tumor growth more effectively than CMV-BikDD. Although CMV-BikDD consistently and significantly prolonged the median survival time of mice compared with the control (40 ± 3 days versus 30 ± 2 days, $p < 0.0003$), C-VISA-BikDD prolonged mouse survival even

more effectively than CMV-BikDD ($p < 0.01$) (Figure 5B). In the C-VISA-BikDD treatment group, signal was undetectable in five of eight mice at 60 days after treatment; at 14 months, those five mice still showed no detectable signal, suggesting that their tumors had been eradicated. Apoptosis induction by C-VISA-BikDD was more potent than that by CMV-BikDD ($p < 0.002$) (Figure 5C). Therefore, the therapeutic efficacy of C-VISA-BikDD can be demonstrated both in an immunodeficient mouse model with human pancreatic tumor cells and in an intact immunocompetent mouse model with murine pancreatic tumors.

Owing to the highly aggressive nature of Panc02 cells, orthotopic Panc02 tumors easily invade and metastasize to local and distant sites (Yan et al., 2006). To investigate whether C-VISA-BikDD could inhibit invasion or metastasis of Panc02 tumors, mice treated as described in the previous section were subjected to imaging in vivo and ex vivo at 28 days after the first treatment. Ex vivo imaging showed that Panc02 tumors in the pancreas of control mice were the largest (2.5 ± 0.5 g) and also invaded or metastasized to the peritoneal omentum, intestinal mesentery, liver, spleen, kidneys, bladder, lungs, and bone (metastatic tumors ranged from 50 mg to 1.5 g) (Figure 5D). Tumors in the pancreas of CMV-BikDD-treated mice were much smaller (50 ± 12 mg), and only a few very small tumors were found in the surrounding organs. Almost no signal was detected in the abdominal cavity of C-VISA-BikDD-treated mice, indicating that the treatment prevented metastases from developing (Figure 5D).

C-VISA-BikDD Produces Virtually No Acute Toxicity Compared With CMV-BikDD

To characterize whether treatment with C-VISA-BikDD is safer than CMV-BikDD in preclinical experiments, we evaluated systemic toxic effects in the female C57BL/6 mice that had been used for the syngeneic pancreatic tumor experiments (Figure 6). Single doses of 2.5 or 5 mg plasmid DNA/kg mouse weight were given by tail-vein injection in a volume of 100 μl of DNA:liposome complexes. Ten of ten (100%) mice treated with a single 5 mg/kg (100 μg per mouse) dose of CMV-BikDD died the next day. However, only two of ten mice treated with a single 5 mg/kg dose of C-VISA-BikDD died during the first 2 days and the surviving mice remained alive for more than 3 months without any obvious symptoms when the experiment was terminated (Figure 6A, left panel and data not shown) ($p < 0.004$ versus CMV-BikDD). All of the animals were alive with no evidence of toxic effects after treatment with a single 2.5 mg/kg (50 μg per mouse) dose of C-VISA-BikDD (Figure 6A, right panel). Blood samples were collected from all living mice after treatment with a single 50-μg dose of C-VISA-BikDD or CMV-BikDD, and serum levels of liver aspartate aminotransferase (AST), alanine aminotransferase (ALT), and blood urea nitrogen (BUN) were measured. Treatment with CMV-BikDD generated 6.5- and 11.7-fold increases in AST levels, and 25- and 24-fold increases in ALT levels on day 1 and day 2, respectively, indicating that CMV-BikDD caused severe acute liver toxicity. However, treatment with C-VISA-BikDD did not increase the levels of AST or ALT, indicating minimal (if any) liver toxicity in the surviving mice (Figure 6B). BUN levels were not elevated at any measurement time (data not shown), indicating a lack of nephrotoxicity of both CMV-BikDD and C-VISA-BikDD. Hematoxylin and eosin staining (H&E) showed that mice treated with C-VISA-BikDD had no pathological changes in major organs relative to the control mice. Notably, systemic administration of C-VISA-BikDD plasmid in a liposomal complex at a therapeutic dose of 0.75 mg/kg (15 μg/mouse) resulted in no obvious toxic effects in C57BL/6 or BALB/c *nu/nu* mice, i.e., no elevated liver enzymes, moribund behavior, or death, and the mice looked healthy during the course of the experiments (data not shown).

To further investigate whether there is any evidence of underlying acute pancreatitis in C-VISA-treated mice, we performed the toxicity experiment in C57BL/6 mice by measuring pancreatic exocrine enzyme levels, H&E and TUNEL analysis. Cerulein-induced acute pancreatitis was used as positive control. As illustrated in Figure 6C, no differences were observed at the levels of serum amylase ($p = 0.6$) and pancreatic active trypsin activity ($p = 0.1$) between the C-VISA-BikDD-treated mice and the C-VISA control mice (Ctrl). However, treatment with CMV-BikDD induced a significant increase in the levels of serum amylase ($p < 0.001$ versus Ctrl) and pancreatic active trypsin activity ($p < 0.002$ versus Ctrl). As expected in the positive control group, treatment with supraphysiologic amount of cerulein induced both elevated levels of serum amylase and pancreatic active trypsin activity (Figure 6C). In addition, histological examination of the pancreas from mice treated with C-VISA-BikDD, CMV-BikDD and C-VISA control vector, showed no evidence of parenchymal edema, pancreatic epithelial vacuolization and necrosis/apoptosis, and inflammatory cell infiltration; however, there was an overt onset of acute pancreatitis induced by cerulein. Furthermore, no TUNEL-positive cells appeared in the acinar and ductal cells of the pancreata of mice treated with C-VISA-BikDD as compared with the control mice treated with C-VISA, in contrast to apoptotic positive cells of the pancreata of mice treated with CMV-BikDD (1.5% TUNEL-positive cells) and with cerulein (4.5% TUNEL-positive cells) (Figure 6D). Taken together, treatment with C-VISA-BikDD produces virtually no systemically acute toxicity (Figures 6A and 6B) or acute pancreatitis (Figures 6C and 6D).

DISCUSSION

A key determinant of safe and effective treatment for cancer is the ability to target cancer cells both at the site of the primary tumor and at distant metastatic sites (Zhou and Bartek, 2004). Transductional targeting and transcriptional targeting are two primary approaches that are used. Transcriptional targeting is of particular importance in liposome-based systemic gene delivery (Qiao et al., 2002; Reynolds et al., 2001). With the goal of developing a robust and pancreatic-cancer-specific vector, we previously identified the CCKAR promoter as a

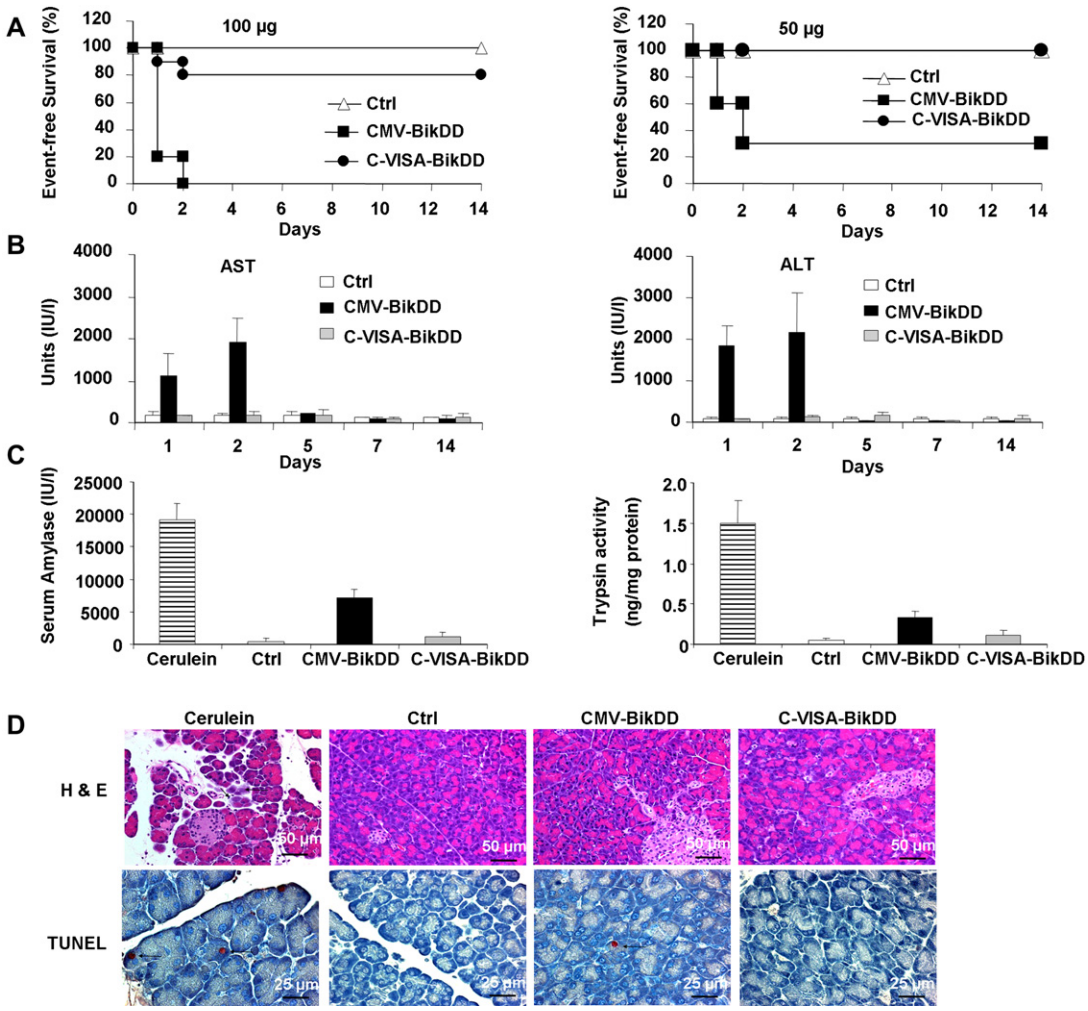

Figure 6. C-VISA-BikDD Has No Systemically Acute Toxicity Compared With CMV-BikDD in Mice

(A and B) C-VISA-BikDD has no systemically acute toxicity compared with CMV-BikDD. (A) Kaplan-Meier survival analysis. Female C57BL/6 mice were given single doses of 100 μg (left panel) or 50 μg (right panel) plasmid DNA in a liposomal complex via the tail vein. (B) Kinetics of serum levels of AST and ALT after a single intravenously injection of 50 μg liposomal plasmid DNA. Error bars indicate SD; AST, aspartate aminotransferase; ALT, alanine aminotransferase.

(C and D) C-VISA-BikDD has no acute pancreatic toxicity compared with CMV-BikDD and cerulein treatment in mice. (C) Serum amylase (left) and pancreatic trypsin (right) activity were shown. Data are means minus the basal level of mice treated with normal saline (NS). Error bars indicate standard deviation. (D) Morphologic (H&E) and apoptosis (TUNEL) analysis of pancreas from mice treated with cerulein. Arrows indicate examples of necrotic cells in cerulein group (H&E) or apoptotic cells in cerulein and CMV-BikDD groups; arrow head indicates an example of inflammatory cell infiltration in cerulein group (H&E). The percentage of apoptotic cells were measured by positive TUNEL staining from 10 fields.

pancreatic-cancer-specific promoter (Li et al., 2006). CCKAR expression is known to be upregulated in the ductal cells of the human PDAC as compared to the normal pancreatic cells by multiple independent groups (Goetze et al., 2000; Jang et al., 2005; Moonka et al., 1999; Weinberg et al., 1997), except for one (Reubi et al., 2003). To clarify this issue, we also performed the experiments. The results supported the former (Figure S1A). The truncated CCKAR promoter, ranging from −726 to +1, and our engineered C-VISA showed undetectable activity or significantly lower activity than the CMV promoter, in cancer cells of nonpancreatic origin in vitro (Figure 1D) and in normal mouse tissues in vivo (Figure 2). C-VISA is a composite that contains three basic elements: the CCKAR promoter, the TSTA system, and the WPRE sequence. C-VISA-BikDD selectively controls expression of BikDD in PDAC, involving four steps as illustrated in Figure 7: (1) CCKAR drives the expression of the GAL4-VP2 (two copies of VP16) fusion protein selectively in PDAC but not in normal cells; (2) GAL4-VP2, which contains a yeast GAL4 DNA-binding domain and a strong transactivation domain derived from HSV-1 VP16, then turns on target gene BikDD mRNA transcripts under the control of GAL4 response elements in a minimal promoter G5E4T recognized by the GAL4 DNA-binding domain within the same plasmid; (3) the BikDD mRNA transcripts contains the

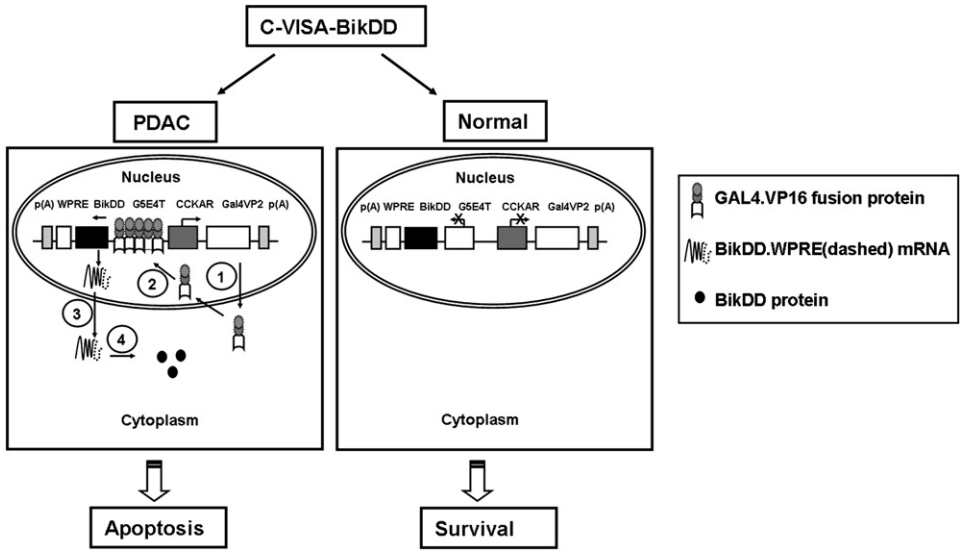

Figure 7. Schematic Diagram of the C-VISA-BikDD System

The C-VISA-BikDD system involves four steps in human PDAC. (1) CCKAR drives the expression of the GAL4-VP2 fusion protein selectively in PDAC but not in normal cells; (2) GAL4-VP2 then turns on target gene BikDD mRNA transcripts; (3) the BikDD mRNA transcripts contains the WPRE element, which stabilizes RNA transcripts; and (4) the stabilized BikDD mRNA transcripts enhance and prolong duration of BikDD protein expression, leading to apoptosis of PDAC cells. For normal cells or normal pancreas, the CCKAR promoter is much less active, resulting in very limited target gene expression and, therefore, cell survival.

WPRE element, which stabilizes RNA transcripts; and (4) the stabilized BikDD mRNA transcripts enhance and prolong duration of BikDD protein expression, leading to apoptosis of PDAC cells. Whereas for normal cells or normal pancreas, the CCKAR promoter is much less active, resulting in very limited target gene expression and therefore cell survival. Thus, C-VISA is much better than C-TSTA or CMV in activity and TEI (Figures 1 and 2). The pancreatic-cancer-specific index of C-VISA was significantly higher than that of the CMV promoter (47.7 versus 0.005), representing a 9500-fold improvement. The VISA system is also a versatile tool to boost other tissue- or cancer-specific promoters for developing promising therapeutics for other diseases.

One of the major technical challenges of nonviral gene delivery approaches is the inefficiency of systemic delivery and transgene expression (Conwell and Huang, 2005; Glover et al., 2005; Lo et al., 2005; Qiao et al., 2002). Extruded DOTAP:cholesterol liposomes can complex with plasmid DNA to form turbid colloidal particles with a mean size of 405 nm in diameter and a half-life of at least 5 hr in circulation, leading to enhanced expression of transgene in most tissues (Templeton et al., 1997). Here, we complexed extruded DOTAP:cholesterol liposomes with reporter plasmid DNA in which the luciferase gene is under the control of the robust C-VISA vector. After systemic delivery of C-VISA-Luc:liposome complexes in vivo in multiple orthotopic models, monitoring with the IVIS imaging system and traditional methods showed that transgene expression was effectively targeted to the pancreatic tumors. The high level of in vivo target luciferase expression (about 22%) (Figure 2F) was obtained in the orthotopic AsPC-1 tumors of mice after a single injection of a liposomal C-VISA-Luc complex.

The highly efficient transgene targeting using C-VISA in DNA:liposome complexes makes it feasible to develop a safe and effective nonviral-mediated gene therapy strategy. Here we rigorously tested the antitumor effects of BikDD driven by C-VISA in plasmid DNA:liposome complexes injected via the tail vein in xenograft and syngeneic orthotopic mouse models by using imaging of live animals and traditional methods. Our findings demonstrated that C-VISA-BikDD induced apoptosis of targeted pancreatic tumor cells, repressed tumor growth, and prolonged mouse life span more effectively than CMV-BikDD in both models. Also worthwhile to mention is that the tumor suppressor gene *p53* is known to be inactivated by mutations in 40%–75% of pancreatic adenocarcinomas (Bardeesy and DePinho, 2002; Hingorani et al., 2005; Li et al., 2004). The lack of functional p53 has been reported to be a component of resistance to DNA-damaging agents, resulting in the inhibition of apoptosis (Zhou and Bartek, 2004); indeed, p53-negative AsPC-1 cells are resistant to p53-mediated apoptosis (Rodicker and Putzer, 2003). Our findings showed that treatment with C-VISA-BikDD effectively led to apoptotic death of AsPC-1 cells in vitro and in vivo. More importantly, BikDD expression driven by the C-VISA promoter induced pancreatic-cancer-specific apoptosis in vitro and in vivo in agreement with the selectivity of the C-VISA vector. This specificity was further reflected in the systemic acute toxicity profile. Systemic administration of C-VISA-BikDD was much less toxic than CMV-BikDD in C57BL/6 mice.

Our established orthotopic mouse models and our live animal imaging capability have made it possible for noninvasive, spatiotemporal monitoring of the growth and metastasis of pancreatic tumors. In traditional models of orthotopic pancreatic cancer, monitoring tumor growth, especially the identification of metastases, is difficult even at necropsy. For these studies, we generated two orthotopic pancreatic cancer models, syngeneic Panc02-Luc and xenograft AsPC-1-Luc, in which primary and metastatic tumors glow from the expression of firefly luciferase after injection of D-Luciferin. Our real-time monitoring models not only facilitated the localization of tumors and metastases but also reduced the number of animals required for the studies.

In summary, we have engineered C-VISA, a stringently pancreatic-cancer-specific expression vector that induces longer and stronger transgene expression than the CMV promoter-driven expression vector in vitro and in vivo. C-VISA targets transgene expression to pancreatic cancer in vivo in animal models. Expression of a potent proapoptotic Bik mutant gene (BikDD) driven by C-VISA after systemic liposome-mediated delivery exhibits significant antitumor effects on pancreatic cancer and prolongs survival in multiple orthotopic xenograft and syngeneic mouse models of pancreatic tumors with minimal or no toxic effects. Overall, this study demonstrates the feasibility of C-VISA-BikDD:liposome complexes as a safe and highly effective gene therapy strategy for pancreatic cancer and is worthy of further development into clinical trials. The versatile VISA system can also be applied to other tissue- or cancer-specific promoters for the development of promising therapeutics for other diseases.

EXPERIMENTAL PROCEDURES

Cell Culture

For sources of cell lines and culture media, see the Supplemental Data. All patients provided informed consent with institutional review board approval of all protocols.

Constructs

The constructs including pGL3-CCKAR-Luc-(C-Luc), pGL3-CCKAR-Luc-WPRE (C-P-Luc), pGL3-CCKAR-TSTA-Luc (C-T-Luc), pGL3-CCKAR-TSTA-Luc-WPRE (C-VISA-Luc), pGL3-CMV-Luc (CMV-Luc), pUK21-CMV-BikDD (CMV-BikDD), and pUK21-C-VISA-BikDD (C-VISA-BikDD) were generated according to the standard molecular cloning protocol.

Animal Models of Pancreatic Cancer, Delivery of Plasmid DNA and Imaging Analysis

Mice were maintained in a specific pathogen-free environment in compliance with institutional policy and all animal procedures were previously approved by the appropriate institutional review boards. The subcutaneous and orthotopic models were established as described previously (Wen et al., 2001; Xie et al., 2001). The growth and metastasis of tumors were monitored in real time with the IVIS imaging system, equipped with Living Imaging software (Xenogen, Alameda, CA). For details on the treatments and analysis, see the Supplemental Data.

Imaging and Quantification of Bioluminescence Data

Mice were anesthetized with a mixture of oxygen and isoflurane (Inhalation Anesthesia System; Matrix Medical, Orchard Park, NY) and intraperitoneally injected with 100 μl of D-luciferin (Xenogen; 30 mg/ml in phosphate-buffered saline [PBS]). Ten minutes after injection, mice underwent imaging with the IVIS Imaging System (Xie et al., 2004). Imaging parameters were maintained for comparative analyses. The imaging results were analyzed with the manufacturer's software (Living Imaging, version 2.5; Xenogen). A region of interest (ROI) was manually selected over relevant regions of signal intensity. The ROI was kept constant, and the intensity was recorded as the maximum number of photon counts within an ROI (Iyer et al., 2001; Xie et al., 2004). In vivo cell imaging was performed 5 min after the addition of D-luciferin at a final concentration of 5 ng/ml. Bars indicate standard error (SEM).

Analysis of Acute Toxic Effects Induced by Systemic Administration in Mice

C57BL/6 mice were studied for evidence of acute toxic effects induced by systemic administration of DNA:liposomal complexes. Levels of serum AST, ALT, and BUN were measured at the biochemistry laboratory in the Department of Veterinary Medicine and Surgery. Serum amylase activity was determined using the Phadebas Amylase Test Kit (Magle Life Sciences, Lund, Sweden). The pancreatic tissue was homogenized and assayed for active trypsin (Lugea et al., 2006). Trypsin activity was calculated according to a standard curve from purified trypsin (Sigma). Shown in Figure 6C are the means subtracted from the basal levels of serum amylase and trypsin activity, respectively, of the NS controls.

Statistical Analyses

Analysis of variance was used to compare the differences among the treatment groups. Survival rates were analyzed by log-rank test (Mantel-Cox test) using SSPS 12.1 software. The significance level was set at $p < 0.05$.

Additional Experimental Procedures

Detailed descriptions are provided in the Supplemental Data.

Supplemental Data

The Supplemental Data include Supplemental Experimental Procedures and three supplemental figures and can be found with this article online at http://www.cancercell.org/cgi/content/full/12/1/52/DC1/.

ACKNOWLEDGMENTS

We thank Dr. Michael Carey (University of California Los Angeles School of Medicine, Los Angeles, CA) for providing the pGL3-TSTA-Luc vector; Dr. James B. Uney (University of Bristol, Bristol, United Kingdom) for providing the pGEM-3Z-WPRE vector; the biochemistry laboratory in the Department of Veterinary Medicine and Surgery for measuring serum AST, ALT, and BUN; and the Department of Scientific Publications at M.D. Anderson Cancer Center for editing this manuscript. This work was supported by an NIH SPORE grant in Pancreatic Cancer (P20 CA101936), a grant from Topfer Funds (M.-C.H. and J.L.A.), M.D. Anderson Cancer Center Support Grant CA16672, and an AstraZeneca Fellowship (X.X.). The M.D. Anderson Cancer Center has filed patent for the VISA-BikDD expression vector, which has been licensed to the ALchemgen Therapeutics Inc. (ATI). M.-C.H. also owns common stocks of ATI. This work was partially supported by ATI (to M.-C.H.).

Received: August 25, 2006
Revised: March 9, 2007
Accepted: May 11, 2007
Published: July 9, 2007

REFERENCES

Bardeesy, N., and DePinho, R.A. (2002). Pancreatic cancer biology and genetics. Nat. Rev. Cancer *2*, 897–909.

Boyd, J.M., Gallo, G.J., Elangovan, B., Houghton, A.B., Malstrom, S., Avery, B.J., Ebb, R.G., Subramanian, T., Chittenden, T., Lutz, R.J., et al. (1995). Bik, a novel death-inducing protein shares a distinct sequence motif with Bcl-2 family proteins and interacts with viral and cellular survival-promoting proteins. Oncogene *11*, 1921–1928.

Certo, M., Del Gaizo Moore, V., Nishino, M., Wei, G., Korsmeyer, S., Armstrong, S.A., and Letai, A. (2006). Mitochondria primed by death signals determine cellular addiction to antiapoptotic BCL-2 family members. Cancer Cell *9*, 351–365.

Chen, J.S., Liu, J.C., Shen, L., Rau, K.M., Kuo, H.P., Li, Y.M., Shi, D., Lee, Y.C., Chang, K.J., and Hung, M.C. (2004). Cancer-specific activation of the survivin promoter and its potential use in gene therapy. Cancer Gene Ther. *11*, 740–747.

Conwell, C.C., and Huang, L. (2005). Recent advances in non-viral gene delivery. Adv. Genet. *53*, 3–18.

Day, C.P., Rau, K.M., Qiu, L., Liu, C.W., Kuo, H.P., Xie, X., Lopez-Berestein, G., Hortobagyi, G.N., and Hung, M.C. (2006). Mutant Bik expression mediated by the enhanced minimal topoisomerase IIalpha promoter selectively suppressed breast tumors in an animal model. Cancer Gene Ther. *13*, 706–719.

El-Deiry, W.S., Sigman, C.C., and Kelloff, G.J. (2006). Imaging and oncologic drug development. J. Clin. Oncol. *24*, 3261–3273.

Gelovani Tjuvajev, J., and Blasberg, R.G. (2003). In vivo imaging of molecular-genetic targets for cancer therapy. Cancer Cell *3*, 327–332.

Glover, C.P., Bienemann, A.S., Heywood, D.J., Cosgrave, A.S., and Uney, J.B. (2002). Adenoviral-mediated, high-level, cell-specific transgene expression: A SYN1-WPRE cassette mediates increased transgene expression with no loss of neuron specificity. Mol. Ther. *5*, 509–516.

Glover, D.J., Lipps, H.J., and Jans, D.A. (2005). Towards safe, non-viral therapeutic gene expression in humans. Nat. Rev. Genet. *6*, 299–310.

Goetze, J.P., Nielsen, F.C., Burcharth, F., and Rehfeld, J.F. (2000). Closing the gastrin loop in pancreatic carcinoma: Coexpression of gastrin and its receptor in solid human pancreatic adenocarcinoma. Cancer *88*, 2487–2494.

Gross, S., and Piwnica-Worms, D. (2005). Spying on cancer: Molecular imaging in vivo with genetically encoded reporters. Cancer Cell *7*, 5–15.

Han, J., Sabbatini, P., and White, E. (1996). Induction of apoptosis by human Nbk/Bik, a BH3-containing protein that interacts with E1B 19K. Mol. Cell. Biol. *16*, 5857–5864.

Hanahan, D., and Weinberg, R.A. (2000). The hallmarks of cancer. Cell *100*, 57–70.

Hingorani, S.R., Wang, L., Multani, A.S., Combs, C., Deramaudt, T.B., Hruban, R.H., Rustgi, A.K., Chang, S., and Tuveson, D.A. (2005). Trp53R172H and KrasG12D cooperate to promote chromosomal instability and widely metastatic pancreatic ductal adenocarcinoma in mice. Cancer Cell *7*, 469–483.

Iyer, M., Wu, L., Carey, M., Wang, Y., Smallwood, A., and Gambhir, S.S. (2001). Two-step transcriptional amplification as a method for imaging reporter gene expression using weak promoters. Proc. Natl. Acad. Sci. USA *98*, 14595–14600.

Jacob, D., Davis, J.J., Zhang, L., Zhu, H., Teraishi, F., and Fang, B. (2005). Suppression of pancreatic tumor growth in the liver by systemic administration of the TRAIL gene driven by the hTERT promoter. Cancer Gene Ther. *12*, 109–115.

Jaffee, E.M., Hruban, R.H., Canto, M., and Kern, S.E. (2002). Focus on pancreas cancer. Cancer Cell *2*, 25–28.

Jang, J.Y., Kim, S.W., Ku, J.L., Park, Y.H., and Park, J.G. (2005). Presence of CCK-A, B receptors and effect of gastrin and cholecystokinin on growth of pancreatobiliary cancer cell lines. World J. Gastroenterol. *11*, 803–809.

Jemal, A., Siegel, R., Ward, E., Murray, T., Xu, J., and Thun, M.J. (2007). Cancer statistics, 2007. CA Cancer J. Clin. *57*, 43–66.

Li, D., Xie, K., Wolff, R., and Abbruzzese, J.L. (2004). Pancreatic cancer. Lancet *363*, 1049–1057.

Li, Y.M., Wen, Y., Zhou, B.P., Kuo, H.P., Ding, Q., and Hung, M.C. (2003). Enhancement of Bik antitumor effect by Bik mutants. Cancer Res. *63*, 7630–7633.

Li, Z., Ding, Q., Li, Y., Miller, S.A., Abbruzzese, J.L., and Hung, M.C. (2006). Suppression of pancreatic tumor progression by systemic delivery of a pancreatic-cancer-specific promoter driven Bik mutant. Cancer Lett. *236*, 58–63.

Lo, H.W., Day, C.P., and Hung, M.C. (2005). Cancer-specific gene therapy. Adv. Genet. *54*, 235–255.

Lugea, A., Nan, L., French, S.W., Bezerra, J.A., Gukovskaya, A.S., and Pandol, S.J. (2006). Pancreas recovery following cerulein-induced pancreatitis is impaired in plasminogen-deficient mice. Gastroenterology *131*, 885–899.

Moonka, R., Zhou, W., and Bell, R.H., Jr. (1999). Cholecystokinin-A receptor messenger RNA expression in human pancreatic cancer. J. Gastrointest. Surg. *3*, 134–140.

Naumann, U., Schmidt, F., Wick, W., Frank, B., Weit, S., Gillissen, B., Daniel, P., and Weller, M. (2003). Adenoviral natural born killer gene therapy for malignant glioma. Hum. Gene Ther. *14*, 1235–1246.

Ou-Yang, F., Lan, K.L., Chen, C.T., Liu, J.C., Weng, C.L., Chou, C.K., Xie, X., Hung, J.Y., Wei, Y., Hortobagyi, G.N., and Hung, M.C. (2006). Endostatin-cytosine deaminase fusion protein suppresses tumor growth by targeting neovascular endothelial cells. Cancer Res. *66*, 378–384.

Qiao, J., Doubrovin, M., Sauter, B.V., Huang, Y., Guo, Z.S., Balatoni, J., Akhurst, T., Blasberg, R.G., Tjuvajev, J.G., Chen, S.H., and Woo, S.L. (2002). Tumor-specific transcriptional targeting of suicide gene therapy. Gene Ther. *9*, 168–175.

Reed, J.C. (2003). Apoptosis-targeted therapies for cancer. Cancer Cell *3*, 17–22.

Reubi, J.C., Waser, B., Gugger, M., Friess, H., Kleeff, J., Kayed, H., Buchler, M.W., and Laissue, J.A. (2003). Distribution of CCK1 and CCK2 receptors in normal and diseased human pancreatic tissue. Gastroenterology *125*, 98–106.

Reynolds, P.N., Nicklin, S.A., Kaliberova, L., Boatman, B.G., Grizzle, W.E., Balyasnikova, I.V., Baker, A.H., Danilov, S.M., and Curiel, D.T. (2001). Combined transductional and transcriptional targeting improves the specificity of transgene expression in vivo. Nat. Biotechnol. *19*, 838–842.

Rodicker, F., and Putzer, B.M. (2003). p73 is effective in p53-null pancreatic cancer cells resistant to wild-type TP53 gene replacement. Cancer Res. *63*, 2737–2741.

Sata, N., Klonowski-Stumpe, H., Han, B., Luthen, R., Haussinger, D., and Niederau, C. (1999). Supraphysiologic concentrations of cerulein induce apoptosis in the rat pancreatic acinar cell line AR4–2J. Pancreas *19*, 76–82.

Seethammagari, M.R., Xie, X., Greenberg, N.M., and Spencer, D.M. (2006). EZC-prostate models offer high sensitivity and specificity for noninvasive imaging of prostate cancer progression and androgen receptor action. Cancer Res. *66*, 6199–6209.

Su, Z.Z., Sarkar, D., Emdad, L., Duigou, G.J., Young, C.S., Ware, J., Randolph, A., Valerie, K., and Fisher, P.B. (2005). Targeting gene expression selectively in cancer cells by using the progression-elevated gene-3 promoter. Proc. Natl. Acad. Sci. USA *102*, 1059–1064.

Templeton, N.S., Lasic, D.D., Frederik, P.M., Strey, H.H., Roberts, D.D., and Pavlakis, G.N. (1997). Improved DNA: Liposome complexes for increased systemic delivery and gene expression. Nat. Biotechnol. *15*, 647–652.

Thorne, S.H., Negrin, R.S., and Contag, C.H. (2006). Synergistic antitumor effects of immune cell-viral biotherapy. Science *311*, 1780–1784.

Wang, X.P., Yazawa, K., Yang, J., Kohn, D., Fisher, W.E., and Brunicardi, F.C. (2004). Specific gene expression and therapy for pancreatic cancer using the cytosine deaminase gene directed by the rat insulin promoter. J. Gastrointest. Surg. *8*, 98–108.

Weinberg, D.S., Ruggeri, B., Barber, M.T., Biswas, S., Miknyocki, S., and Waldman, S.A. (1997). Cholecystokinin A and B receptors are differentially expressed in normal pancreas and pancreatic adenocarcinoma. J. Clin. Invest. *100*, 597–603.

Wen, Y., Yan, D.H., Wang, B., Spohn, B., Ding, Y., Shao, R., Zou, Y., Xie, K., and Hung, M.C. (2001). p202, an interferon-inducible protein, mediates multiple antitumor activities in human pancreatic cancer xenograft models. Cancer Res. *61*, 7142–7147.

Wesseling, J.G., Yamamoto, M., Adachi, Y., Bosma, P.J., van Wijland, M., Blackwell, J.L., Li, H., Reynolds, P.N., Dmitriev, I., Vickers, S.M., et al. (2001). Midkine and cyclooxygenase-2 promoters are promising for adenoviral vector gene delivery of pancreatic carcinoma. Cancer Gene Ther. *8*, 990–996.

Xie, X., Luo, Z., Slawin, K.M., and Spencer, D.M. (2004). The EZC-prostate model: Noninvasive prostate imaging in living mice. Mol. Endocrinol. *18*, 722–732.

Xie, X., Zhao, X., Liu, Y., Young, C.Y., Tindall, D.J., Slawin, K.M., and Spencer, D.M. (2001). Robust prostate-specific expression for targeted gene therapy based on the human kallikrein 2 promoter. Hum. Gene Ther. *12*, 549–561.

Yan, Y., Rubinchik, S., Wood, A.L., Gillanders, W.E., Dong, J.Y., Watson, D.K., and Cole, D.J. (2006). Bystander effect contributes to the antitumor efficacy of CaSm antisense gene therapy in a preclinical model of advanced pancreatic cancer. Mol. Ther. *13*, 357–365.

Zhang, L., Johnson, M., Le, K.H., Sato, M., Ilagan, R., Iyer, M., Gambhir, S.S., Wu, L., and Carey, M. (2003). Interrogating androgen receptor function in recurrent prostate cancer. Cancer Res. *63*, 4552–4560.

Zhou, B.B., and Bartek, J. (2004). Targeting the checkpoint kinases: Chemosensitization versus chemoprotection. Nat. Rev. Cancer *4*, 216–225.

Zou, Y., Peng, H., Zhou, B., Wen, Y., Wang, S.C., Tsai, E.M., and Hung, M.C. (2002). Systemic tumor suppression by the proapoptotic gene bik. Cancer Res. *62*, 8–12.

Zufferey, R., Donello, J.E., Trono, D., and Hope, T.J. (1999). Woodchuck hepatitis virus posttranscriptional regulatory element enhances expression of transgenes delivered by retroviral vectors. J. Virol. *73*, 2886–2892.